Available online at www.eccomasproceedia.org
Eccomas Proceedia COMPDYN (2023) 5242-5257

ECCOMAS
Proceedia

COMPDYN 2023
9th ECCOMAS Thematic Conference on
Computational Methods in Structural Dynamics and Earthquake Engineering
M. Papadrakakis, M. Fragiadakis (eds.)
Athens, Greece, 12-14 June 2023

TYPOLOGICAL FRAGILITY ASSESSMENT OF PRESTRESSED CONCRETE GIRDER BRIDGES SUBJECTED TO TRAFFIC LOADS AFFECTED BY CORROSION

Alessandro Nettis[1], Andrea Nettis[1], Sergio Ruggieri[1] and Giuseppina Uva[1]

[1] Department of Civil, Environmental, Land, Building Engineering and Chemistry,
Polytechnic University of Bari, via E. Orabona 4, 70125, Bari, Italy
e-mail: {alessandro.nettis, andrea.nettis, sergio.ruggieri, giuseppina.uva}@poliba.it

Abstract

Most of the Italian roadway bridges, built from 60s to 80s, are simply supported, girder-type, prestressed concrete bridges. After at least 50 years of service life, material degradation and functional obsolescence problems are coming out leading to the need for evaluating bridge vulnerability to natural and anthropic hazards. Particularly, this study aims at investigating the structural response to traffic loads of different typologies belonging to this bridge class. In this study, geometric and material random variables are assumed to simulate inter-class property variability and statistical sampling techniques are used to randomly generate bridge realisation for each investigated bridge typology. A simplified traffic load analysis is performed, subjecting each bridge realisation to various traffic load models (TLMs) proposed by the current Italian building code. Particularly, different post-tensioned tendon corrosion scenarios are assumed, evaluating the variation in response. Fragility curves are built for each bridge typology for each corrosion scenario and results are discussed with a view to prioritisation in the large-scale assessment of existing prestressed concrete bridge class.

Keywords: Prestressed bridges, traffic loads, post-tensioning, fragility assessment, corrosion.

ISSN:2623-3347
Peer-review under responsibility of the organizing committee of COMPDYN 2023.
doi: 10.7712/120123.10797.21003

1 INTRODUCTION

The structural performance of bridges under traffic loads and natural hazards affects the serviceability and safety of transportation networks. Recent bridge collapses [1, 2] proved that these tragic events can lead to huge direct losses, mainly related to casualties, together with economic losses, involving significant transport disruptions affecting large urban and industrial contexts, reparation or replacement costs. The structural safety of bridges can be threatened by ageing, material deterioration and human-related and natural hazards. Currently, extensive bridge assessments are required by transportation managers to evaluate the performance of these structures under actions induced by natural hazards, which, generally, were not included in past design codes. Particularly, several research studies address refined and simplified methodologies to calculate fragility and risk (e.g. direct and indirect losses) considering seismic actions [3, 4] and floods [5]. Another source of fragility for existing bridges is related to service traffic loads [6–8], which are more severe in terms of number and mass of vehicles with respect to the past. Indeed, most of the existing bridges were designed considering old design traffic load schemes which may be inadequate compared to the current traffic demand. In recent literature studies, Fiorillo et al. [6] use real field truck data to perform fragility analysis of existing bridges considering overweight traffic loads. Miluccio et al. [7] characterise statistical distributions of significant geometric and structural variables for the general class of existing prestressed concrete girder superstructures and perform fragility analysis considering traffic loads.

In European countries, many existing bridges built in the post-war period exhibit severe degradation conditions caused by aggressive environmental agents together with inadequate durability requirements of materials and structural details. Material deterioration should be accounted for during on-site visual inspections for condition rating [9] and for defining targeted network-scale prioritisation of retrofit interventions [10]. Corrosion of prestressing steel strands or wires is considered one of the main causes of capacity degradation of prestressed concrete girder bridges with pre-tensioned and post-tensioned tendons. Particularly, in girders characterised by post-tensioned tendons, corrosion of strands may be triggered by corrosive agents penetrating anchorages and enhanced by construction errors such as incomplete grouting causing voids in the ducts. As evidenced by recent collapses of bridges in Italy [11, 12], corroded tendons may involve significant loss of structural capacity under gravity loads and cause structural failure. Corrosion effects on internal tendons and presence of voids inside the ducts cannot be detected by bridge inspectors via simple visual inspections. Indeed, according to guidelines developed in Italy [13] and United States [14], the condition rating of prestressed girders characterised by post-tensioned tendons requires special inspections in which non-destructive and destructive non-invasive tests are used to detect voids and identify corroded tendons inside the ducts.

Transport network managers are in charge of performing extensive surveys and assessments considering the large amount of prestressed concrete girder bridges equipped with post-tensioned internal tendons built in past decades. In this context, transport authorities' operators require efficient procedures for evaluating the corrosion-induced potential loss of structural capacity for existing bridges. These procedures should accurately and efficiently account for the relevant significance of the epistemic uncertainty commonly affecting the safety assessment, intending to prioritise critical structures to be subjected to refined diagnostic campaigns, assessment and retrofit.

This study investigates the fragility of prestressed concrete girder bridges subjected to traffic loads considering tendon corrosion. A probabilistic assessment methodology is used to evaluate the failure probability under traffic loads. The propagation of epistemic uncertainty

affecting geometric and structural parameters in results is considered through statistical sampling techniques. In this study, the methodology is used to investigate the structural safety of nine different bridge superstructure typologies. Results can be adopted to guide operators for cases within the investigated typologies. However, the same methodology can be similarly applied to investigate other case-study bridges in practice.

2 METHODOLOGY FOR FRAGILITY ANALYSIS

In this section, the adopted methodology for fragility analysis considering the involved uncertain parameters is described (Figure 1). It is worth specifying that a set of different prestressed concrete girder bridge typologies are considered in the study, whose characteristics are specified in section 3.1. In the following, the statistical sampling technique, the simplified modelling and analysis to calculate failure datasets and the algorithm to achieve fragility curves are presented.

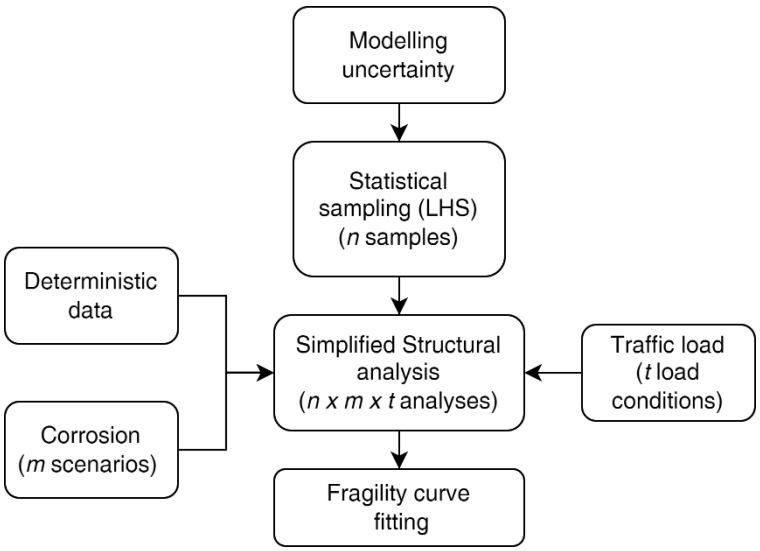

Figure 1: Flowchart for fragility analysis

2.1 Modelling uncertainties

Geometric and mechanical parameters affecting the structural safety assessment of the investigated bridge typologies are required as input for the proposed approach. In practical application, only few geometric parameters are deterministically modelled since these have poor influence in response computation or have low variability within the considered bridge typologies. They can be accurately deduced by design blueprints or by using on-site measurements [15]. Conversely, the determination of accurate values for other geometric structural variables and mechanical parameters of materials would require running an appropriate diagnostic campaign based on non-destructive and destructive tests, involving inevitably additional effort in the assessment process. In this methodology, such variables are assumed as epistemic uncertainties (i.e., deriving from an imperfect initial knowledge [16]) and two kinds of variables, a set of independent variables and few dependent variables through regression models, are considered. Independent variables are represented by random variables following appropriate statistical distributions. Several studies provide statistical distributions and regression models derived from statistical analysis for parameters affecting the probabilistic structural assessment of existing bridges [7, 17, 18].

After the definition of deterministic and probabilistic independent and dependent variables, the Latin Hypercube Sampling (LHS) [19] is used as a statistical sampling technique for the random generation of a population of bridge model realisations. Particularly LHS generation is applied to get random samples of independent variables. Once these are available, dependent variables are inferred through regression models. The model realisations exhibit the same deterministic parameters, but different uncertain parameters depending on the associated statistical distributions and regression models. The LHS is widely used in literature for the probabilistic seismic analysis of both single or portfolios of bridges (e.g. [20, 21]) and is usually preferred over the standard Monte Carlo technique since it requires less computational effort and ensures more accurate sampling from a random variable population. In the LHS framework, the cumulative distributions of the m random variables X_j $(j = 1,2,\dots,m)$ are divided into N equal probability intervals (stratification of the input), where N is the target number of realisations. For the characterisation of each realisation, a single value is randomly extracted from each interval. The output samples are N vectors of size m (i.e., N bridge realisations), in turn, composed of values randomly paired under the assumption that these belong to different intervals. At the end of the sampling process, convergence in statistics should be checked to reach a number of model realisations representative of the real distribution and convenient in terms of computational effort. To do it, a sensitivity analysis [22] is carried out, setting the results obtained from a large set of realisations as a benchmark, and getting different analysis results obtained from smaller sets of bridge realisations. For each number of model realisations, the relative error compared to benchmark results is computed. The desired number of realisations is derived, considering a sample size which ensures that the relative error remains below an imposed threshold. At the end of the process, each realisation is deterministically analysed by using a practical structural analysis approach.

2.2 Simplified structural analysis

The simplified modelling and analysis strategy adopted in this study is suitable for the structural assessment of a simply supported superstructure. Particularly, the so-called Courbon-Albenga method [23] is used for calculating maximum flexure and shear demands for the girders of a given bridge grillage superstructure. According to this method, an infinite flexural stiffness of the transverse diaphragms and a negligible torsional stiffness of the girders is assumed. Under these assumptions and regardless of the position of the diaphragms, the transverse distribution of a given load on the deck among the different girders can be simulated by using distribution coefficients depending only on the number and position of the girders.

Gravity loads in terms of self-weight of the bridge elements and non-structural components are simulated by using uniformly distributed loads. Traffic loads are modelled by adopting the load schemes (tandem plus distributed loads) provided by Eurocode 1-Part 2 [24]. For each model realisation, the demand parameters extracted from the analysis are the maximum bending moment, registered at mid-span, and the maximum shear demand, registered at the support, for the edge girder. The number and arrangement of loaded traffic lanes to be considered in the analysis are defined in such a way as to maximise the flexural and shear demand for the edge girder.

For each model realisation, the demand parameter for flexure and shear, calculated as above, is compared with the corresponding capacity.

2.3 Capacity modelling

As far as capacity is concerned, flexure and shear behaviours are modelled as follows. Mild and prestressing steel areas are modelled as lumped in their centroids within the considered cross-section. For the assessment of the girder capacity, an effective width of the slab equal to the width of the top flange of the beam is assumed.

The computation of the ultimate bending moment strength M_R is based on the following assumptions suggested by the codes [25, 26]: 1) plane cross-sections and perfect steel-concrete bonding after flexural deformation; 2) stress-block model for concrete constitutive law in compression and ultimate concrete compressive strain equal to 0.35%; 3) elastic-perfectly plastic behaviour for mild and prestressing steel.

Generally, the flexure capacity calculation requires the computation of prestressing tendon area in balanced rupture hypothesis, i.e., failure due to simultaneous attainment of ultimate compression strain for upper concrete fibre and yielding tensile strain for mild and prestressing steel. This is necessary for distinguishing between fragile and ductile flexural failures of the analysed transverse section, leading to different ways of ultimate capacity calculation.

For the sake of brevity, it is worth specifying that, for appropriate design of prestressed girders, a ductile failure can be considered. In this case, the computation of ultimate bending is performed through the following equation:

$$M_R = \left(A_{sp} f_{p,01} + A_s f_y\right) z \tag{1}$$

where z is the internal lever arm, depending on the neutral axis position. Concerning shear capacity, the following equation is considered:

$$V_R = 0.7 b_w d \sqrt{f_{ct}^2 + \sigma_{cp} f_{ct}} \tag{2}$$

where b_w is the girder web width; d is the distance of the reinforcing steel from the top compression side (equal to girder height minus concrete cover); f_{ct} is the concrete tensile strength; σ_{cp} is the average compressive concrete stress due to residual prestressing action σ_{sp}. This formulation is derived from Eurocode 2 [26] and retains for prestressed concrete beam members in uncracked configuration.

The influence of tendon corrosion in the abovementioned capacity models is modelled through a percentage reduction of prestressing area proportional to a given corrosion degree defined according to Yu et al. [27]. The influence of corrosion degree on significant tendon mechanical properties is, additionally, modelled according to the study by Yu et al. [27].

2.4 Fragility analysis

In this study, fragility curves express the probability of failure for a given intensity of traffic loads. The failure is achieved for either flexure or shear demand exceeding the corresponding capacity. This sub-section describes the approach for calculating fragility curves, which is developed based on the multi-stripe seismic fragility analysis approach according to Baker [28] and, subsequently, applied by Miluccio et al. [7] for traffic loads.

First, each bridge model realisation is analysed considering increasing value of the traffic load. For this purpose, each realisation is analysed for a set of traffic load scenarios in which the traffic load scheme is multiplied by a factor α ranging from 0 to 2.8 considering an increasing load by steps equal to 0.005. In this case, the α parameter is used as load intensity

measure (IM) for the fragility analysis. Particularly, such a range is considered to get both flexural and shear failures for most of the generated model realisations, as explained in Section 4. For each load step, the demand-to-capacity ratio is derived, considering both flexure and shear demand (DCR_f and DCR_s, respectively). Failure is achieved when:

$$DCR_t = max\left(DCR_f, DCR_s\right) \geq 1 \tag{3}$$

This process is repeated for all the N model realisations included within the whole model population generated via LHS.

The output of this analysis consists of N values of demand-to-capacity ratio collected for each load multiplier of the traffic load scheme described in sub-section 2.2. For each load scenario, the probability of failure conditioned to a load multiplier $P[failure|\alpha]$ is calculated as the ratio between the number of realisations associated with failure N_{fail} ($DCR_t \geq 1$) and the total size N of the model population (Equation (4)).

$$P[failure|\alpha] = P[DCR_t \geq 1|IM = im] = N_{fail}/N \tag{4}$$

Finally, the final fragility function is derived by fitting a lognormal cumulative distribution to the dataset of $P[failure|\alpha]$ related to the considered load scenarios by using the maximum likelihood method [28].

To investigate the influence of tendon corrosion on the fragility of a single bridge typology, fragility functions are calculated for several corrosion scenarios. A comparison between the achieved dataset of fragility curves allows for quantifying the variation in probability of failure for the variation in the intensity of tendon corrosion.

The entire process is then repeated for different bridge typologies, with different values of span length and beam number of the deck.

3 DESCRIPTION OF CASE-STUDY BRIDGE SUPERSTRUCTURES

3.1 Case studies

Different prestressed girder highway bridge typologies, assumed typical of bridges built between 1965 and 1970, are analysed in this study as case studies.

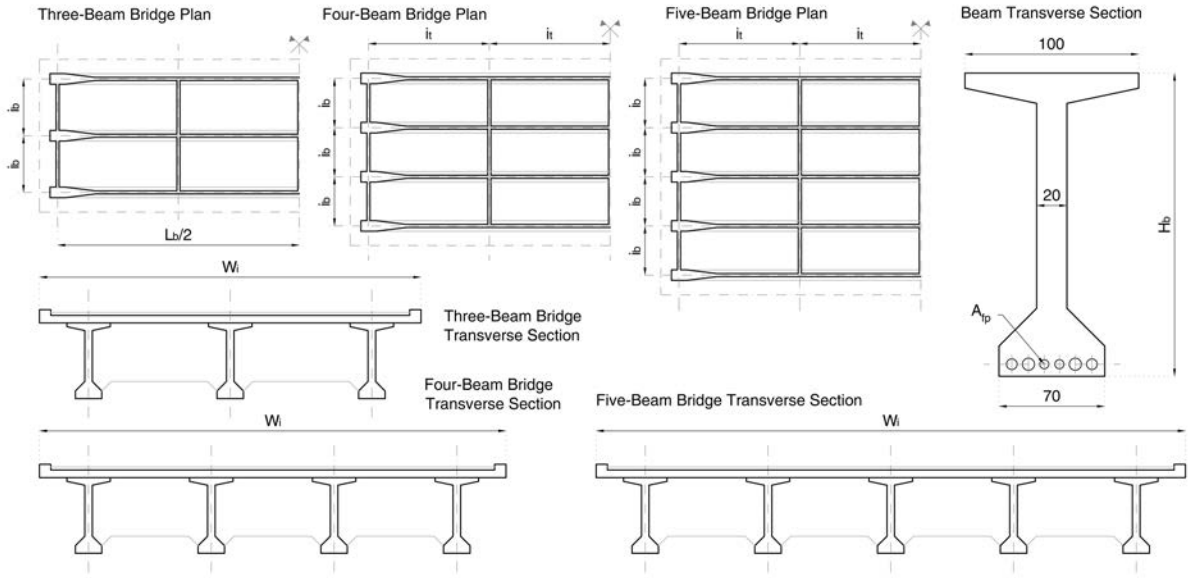

Figure 2: Case-study characteristics

Particularly, nine typologies are obtained, considering: 1) three different values of beam number of the deck (from three to five) and 2) three different values of span length (a short-span typology equal to 15 m, a medium-span typology equal to 35 m and a long-span typology equal to 55 m). These exhibit structural and constructive characteristics representative of the widespread class of simply supported post-tensioned girder bridges in Italy designed in ’60 and ’70 decades (Figure 2). Bridges exhibit multiple simply supported grillage superstructures having repetitive characteristics. The superstructure of each typology is composed of a varying number of girders with a reinforced concrete deck having a total width dependent on the spacing between the girders, which in turn depends on the beam height and the span length. For each case, the girder height varies with the span length and prestressed diaphragms guarantee the transverse load distribution among the girders of the same superstructure. Those components ensure the validity of the assumption of infinite bending stiffness of diaphragms compared to the torsional stiffness of the individual girders, for each typology. The girders of the superstructure present a variable number of tendons collected in specific ducts filled with cementitious grouts. The value of prestressing steel area is related to the span length and is computed through the prestressing steel ratio, i.e., the ratio between the prestressing steel area and the tension area of the concrete cross-section, as stated in section 3.2.

Other geometric data and constructive details of the case-study bridge typologies, which are considered deterministic in the following calculations, are shown in Figure 2. Bridge typologies are assumed designed according to the old Italian regulation *Circolare n.384 del 14.02.1962, Norme relative ai carichi per il calcolo dei ponti stradali* [29]. The carriageways of bridges host different values of real traffic lanes, depending on the deck width, subtracted of the total kerb length.

3.2 Uncertainties and corrosion scenarios

In addition to the deterministic input data, according to the methodology described in Section 2, the epistemic uncertainty related to the lack of deterministic knowledge for other parameters essential for the structural analysis, is modelled through statistical distributions

and regression models. In this case, statistical distributions and regression models useful for the purpose of this study are retrieved from the study by Miluccio et al. [7], who collected data on bridges in South Italy and perform statistical analysis to produce statistical distributions for significant structural and constructive parameters. Such distributions and models are listed in Table 1-2. As shown in the tables, two different kinds of variables are considered in this study, a set of independent variables and few dependent ones, derived via statistical distribution or regression models from other variables assumed as predictors.

For parameters whose statistical distributions are not available, the maximum uncertainty is assumed using a continuous uniform distribution. It is worth mentioning that the use of statistical distributions representative of the considered structural typology and geographical contexts is desirable to achieve a reliable simulation of epistemic uncertainty for the analysed case. A general lack of statistical distributions useful for the investigated purpose is registered in Italy. Although statistical distributions from different contexts are used in this study, it is expected that more statistical data about Italian highway bridges will be available in future, improving the reliability of such an approach.

To investigate the influence of the degree of tendon corrosion on structural response, different corrosion scenarios are considered. Each corrosion scenario is associated with a corrosion degree quantified as the (percentage) ratio ξ of the tendon mass considered affected by corrosion and the initial total one. In the adopted methodology, no variation in the distribution of corrosion among the different tendons for a given girder cross-section is considered. This is because the adopted algorithm for section strength calculation considers the entire set of tendons as a single equivalent one with a mass equal to the sum of the tendon mass, (lumped in the tendon system centroid), neglecting their real distribution within the cross-section. Additionally, the variation in corrosion distribution along the girder longitudinal axis is neglected since only significant cross-sections are considered in the following analyses (sub-section 2.2). For each corrosion scenario, the tendon mass loss is associated with the girder cross-sections considered to calculate the DCR (i.e., mid-span for flexure and at the supports for shear), in which the corrosion degree ξ is equal to [0-20-40] % of the initial tendon mass. Thus, an effective percentage of tendon area η respectively equal to [100-80-60] % is considered in section strength computation.

Parameter	Distribution	Parameters	
Mean concrete compressive strength (f_{cm}) [7]	Lognormal	μ = 38.5; COV = 11.4%	MPa
Mean steel tensile strength (f_{ym}) [7]	Lognormal	μ = 451; COV = 7.2%	MPa
Conventional yield strength of prestressing steel ($f_{p,01}$) [7]	Lognormal	μ = 1665; COV = 7.5%	MPa
Slab thickness (s)	Uniform	μ = 0.25; COV = 12.0%	m
Road pavements thickness (h_{bit})	Uniform	μ = 0.14; COV = 24.7%	m
Residual stress level of prestressing steel (σ_{sp})	Uniform	μ = 600; COV = 11.5%	MPa

Table 1: Statistical distributions for independent variables

Parameter	Predictors	Distribution/Regression model	Bounds	
Beam height (H_b)	L_b	Uniform	$[{L_b}/{20}; {L_b}/{15}]$	m
Beam spacing (i_b) [7]	L_b, H_b	$H_b = 0.28 i_b + 0.03 L_b$	-	m
Prestressing steel ratio (ρ_{sp}) [7]	L_b	$\rho_{sp} d_{sp} = 8.16 \cdot 10^{-5} L_b + 1.85 \cdot 10^{-5} L_b^2$	-	-

Table 2: Statistical distributions and regression models for dependent variables

3.3 Sensitivity analysis

When using a random sampling technique as LHS to randomly generate portfolios of bridges, it is important to ensure that convergence in results is achieved. In this study, for reasons related to computational effort and analysis velocity, it is necessary to set the proper sample size to be generated, to guarantee that additional specimens would not alter the statistics of the sample, within a certain tolerance. The level of variability in the capacity of the randomly generated bridge realisations is obviously connected to the variability of material and geometric properties used in the sampling process.

In the present study, a set of 10^5 bridge realisations of the three-beam medium-span typology, i.e., 35 m-span bridge, for three different corrosion degrees, is used as a reference to estimate the mean fragility curve. Because of the very large size of the sample, this fragility curve is assumed to provide the exact solution for the problem.

Subsequently, a number of samples with increasing sizes, from 5 to 500, are produced and their fragility curves are compared with the result obtained with the reference sample size. The comparison is performed in terms of relative error between the medians of the fragility curves, i.e., the relative difference between the fragility curve median of each sample size and the reference one.

This process is repeated several times for different randomly generated samples and for the three different corrosion scenarios. In Figure 3 the results are shown for ten repetitions of sample generation, for two different values of corrosion degree, equal to 40% and 20%. A relative error threshold of 2% is set and a sample size of 250 model realisations turns out to be the best choice. Beyond this sample size, no significant changes are observed in the results within a 2% tolerance. Thus, throughout this study, a sample size of 250 bridge model realisations is used to perform the analyses.

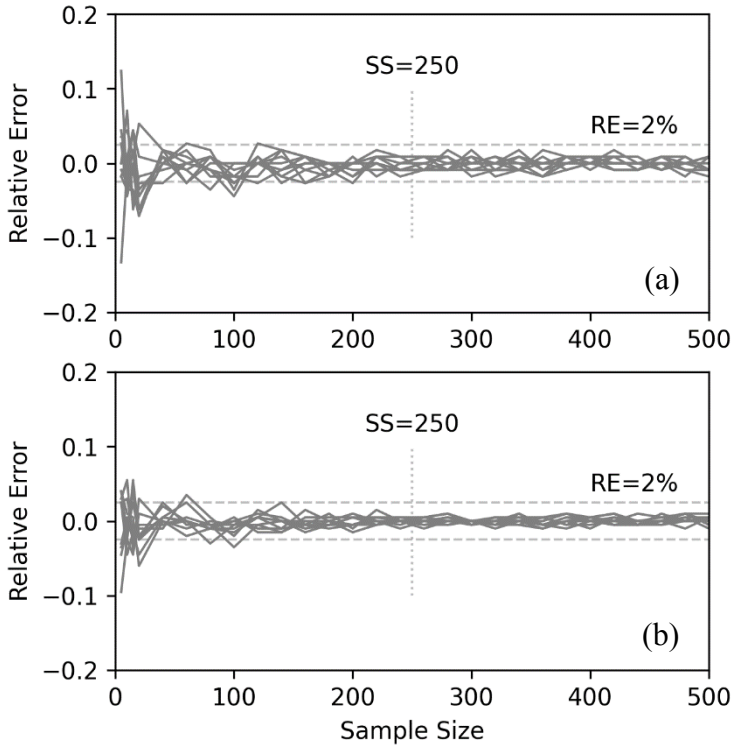

Figure 3: Relative errors as a function of sample size for ten repetitions, (a) 40% of corrosion degree and (b) 20% of corrosion degree

4 DISCUSSION OF RESULTS

In this section, the results and the obtained fragility curves are discussed, mainly focusing on the influence of different corrosion scenarios on bridge response to traffic loads.

Part of the results of the analyses are shown in Tables 3-5; results are given for corrosion degree values of 40, 20 and 0%, and span values of 15, 35 and 55 m, i.e., short-, medium- and long-span typologies.

Bridge type	ξ [%]	Median	Dispersion
Three-beam	40	0.305	0.060
Three-beam	20	0.540	0.076
Three-beam	0	0.765	0.091
Four-beam	40	0.350	0.069
Four-beam	20	0.595	0.085
Four-beam	0	0.840	0.101
Five-beam	40	0.375	0.079
Five-beam	20	0.630	0.101
Five-beam	0	0.880	0.120

Table 3: Fragility parameter corresponding to 15 m-span bridge

Bridge type	ξ [%]	Median	Dispersion
Three-beam	40	0.560	0.135
Three-beam	20	0.990	0.135
Three-beam	0	1.300	0.164
Four-beam	40	0.570	0.151
Four-beam	20	1.010	0.153
Four-beam	0	1.335	0.172
Five-beam	40	0.595	0.160
Five-beam	20	1.060	0.159
Five-beam	0	1.400	0.182

Table 4: Fragility parameters corresponding to 35 m-span bridge

Bridge type	ξ [%]	Median	Dispersion
Three-beam	40	0.705	0.168
Three-beam	20	1.015	0.218
Three-beam	0	1.215	0.237
Four-beam	40	0.695	0.192
Four-beam	20	1.030	0.241
Four-beam	0	1.235	0.261
Five-beam	40	0.710	0.211
Five-beam	20	1.070	0.272
Five-beam	0	1.295	0.287

Table 5: Fragility parameters corresponding to 55 m-span bridge

In general, results show low values of dispersion in fragility curves in most of the cases (Figures 4-6), except for the long-span typology, pointing out a low influence of the considered variables, on average, in the response. Fragility curves highlight that medium- and long-span typologies are adequate for the code-based traffic load up to a 20% of corrosion rate. The short-span typology, on the other hand, seems not adequate for Italian regulation, even with a zero-corrosion value. Therefore, from this study appears that this latter is the typology to be given the most attention in a large-scale analysis. The reasons for this result might lie in the choice of beam height and post-tensioning reinforcement modelling. These

are influenced by the span length value and are lower in case of shorter spans. Thus, future developments need to investigate the problem more in detail, refining the analysis by implementing a simulated design procedure according to the old design code, to further validate the obtained results.

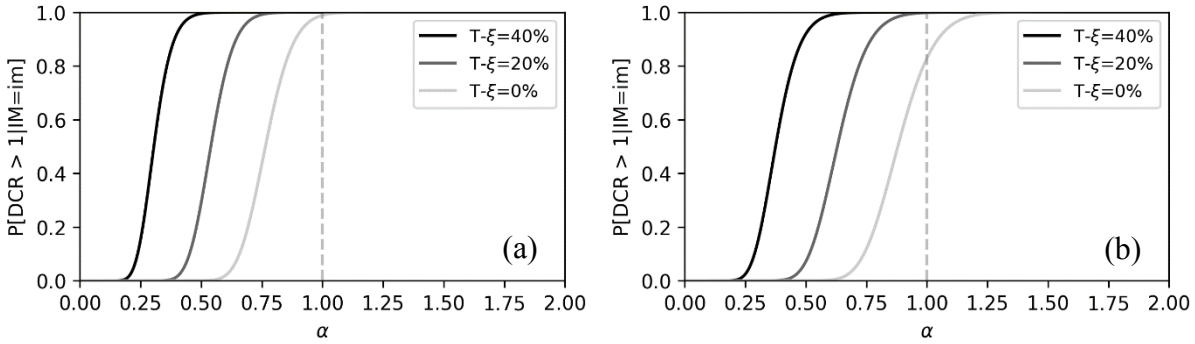

Figure 4: Fragility curves for (a) three- and (b) five-beams, 15 m-span bridge

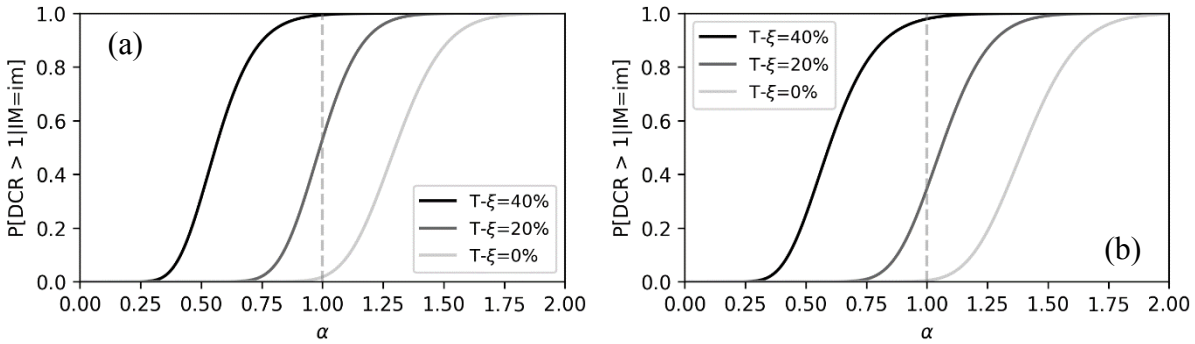

Figure 5: Fragility curves for (a) three- and (b) five-beams, 35 m-span bridge

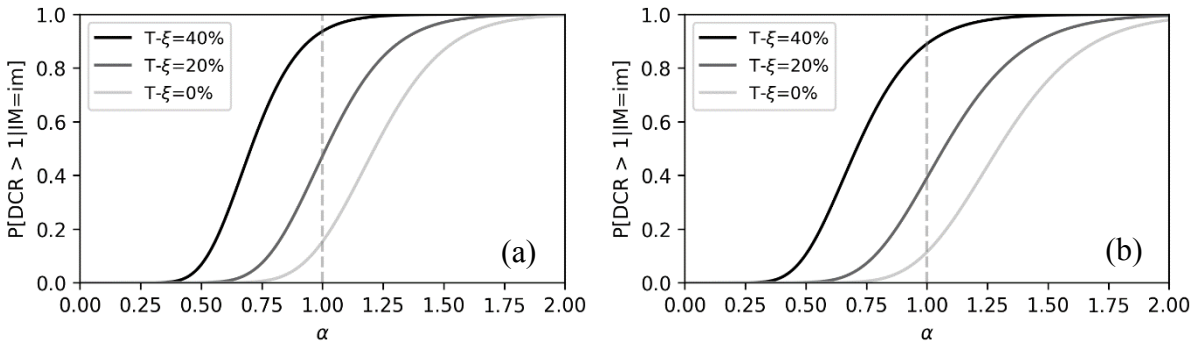

Figure 6: Fragility curves for (a) three- and (b) five-beams, 55 m-span bridge

Span length variation has a strong influence on the structure response to traffic loads. As the span decreases, the structure tends to bear lower loads, for the abovementioned reasons. There is an almost constant response for medium- and long-span typologies. The difference becomes significant when comparing to the short-span ones, which show a decrease in the maximum load-bearing capacity of approximately 40% on average compared to the medium- and long-span, up to a maximum value of 56%, between the long- and short-span, for a three-beam deck typology.

In contrast, the variation in the beam number has a much smaller influence on bridge fragility. There is a slight increase in the load-bearing capacity as the number of beams increases, for the small-span typology the maximum variation in the fragility curve median is obtained for a zero-corrosion value and is equal to 19%, while for the medium- and large-span ones the maximum variation is approximately constant and equal to 7%.

As for the influence of corrosion for the same span value, the response of the bridge is increasingly weaker as the corrosion level increases. By comparing the fragility variation magnitude as the bridge span varies, it can be seen that there is no great difference in terms of fragility curve median variation, which remains approximately constant as span length varies. Indeed, the median variation is about 60% in case of short- and medium-span length, and it drops to around 45% for the longest span. Therefore, there is no evidence of different influence of corrosion among different span typologies, corrosion induces a similar increase in fragility regardless of the span length. It is worth noting that tendon corrosion may determine a significant increase in the bridge fragility, until a 60% of decrease in the fragility curve median value for a corrosion degree increasing from 0 to 40%.

Another consideration concerns the influence of corrosion on bridge response considering the variation of beam number of the deck. In this case, it is clear that there is no evidence of a greater influence of corrosion degree for different values of beam number. Indeed, the variation of the fragility due to varying corrosion levels is nearly constant as the beam number varies and is equal to the abovementioned values, i.e., about a 7% of decrease in fragility curve median values on average for a decreasing beam number.

As far as the dispersion of the fragility curves is concerned, it can be seen that the alteration of corrosion level does not lead to a significant change. The dispersion appears to be roughly constant as the corrosion degree varies, for the same span value and the same number of beams. Conversely, a slight increase in the dispersion is noted as the number of beams increases and it is more pronounced as the span value increases. The latter may be related to the greater variability of the beam height adopted in dependent variable modelling, as this characteristic is related to span value. The greater the span value, the greater the variation of beam height between the two extremes considered. The same applies to the deck width, in turn related to span length and beam height. As these two parameters vary more for greater span values, they result in a greater dispersion in the relative fragility curves.

Failure mode	ξ [%]	Median	Dispersion
Flexural	40	0.375	0.079
Flexural	20	0.630	0.101
Flexural	0	0.880	0.120
Shear	40	1.360	0.079
Shear	20	1.480	0.166
Shear	0	1.585	0.176

Table 6: Flexural and shear fragility parameters for a five-beam 15 m-span bridge

Failure mode	ξ [%]	Median	Dispersion
Flexural	40	0.595	0.160
Flexural	20	1.085	0.174
Flexural	0	1.575	0.199
Shear	40	1.065	0.164
Shear	20	1.250	0.183
Shear	0	1.425	0.197

Table 7: Flexural and shear fragility parameters for a five-beam 35 m-span bridge

Failure mode	ξ [%]	Median	Dispersion
Flexural	40	0.820	0.259
Flexural	20	1.455	0.258
Flexural	0	1.885	0.237
Shear	40	0.815	0.273
Shear	20	1.070	0.293
Shear	0	1.295	0.289

Table 8: Flexural and shear fragility parameters for a five-beam 55 m-span bridge

The fragility analysis for the two different flexural and shear failure modes in Tables 6-8 and in Figure 7 shows that there is no clear dominant failure type for the medium- and long-span typologies. On the contrary, it can be stated that the dominant failure type for short-span decks is related to flexure. As the span increases, the shear failure type becomes increasingly dominant and this is due to the tendon area modelling methods already mentioned. It can also be seen, on the medium- and long-span typologies, that as corrosion increases, flexural failure tends to overwhelm shear failure. This is related to the decrease in the reinforcement considered in the calculation algorithm for flexural strength, a variation which, on the other hand, has a lower influence on shear strength, contributing only to the compression state of the beam cross-section.

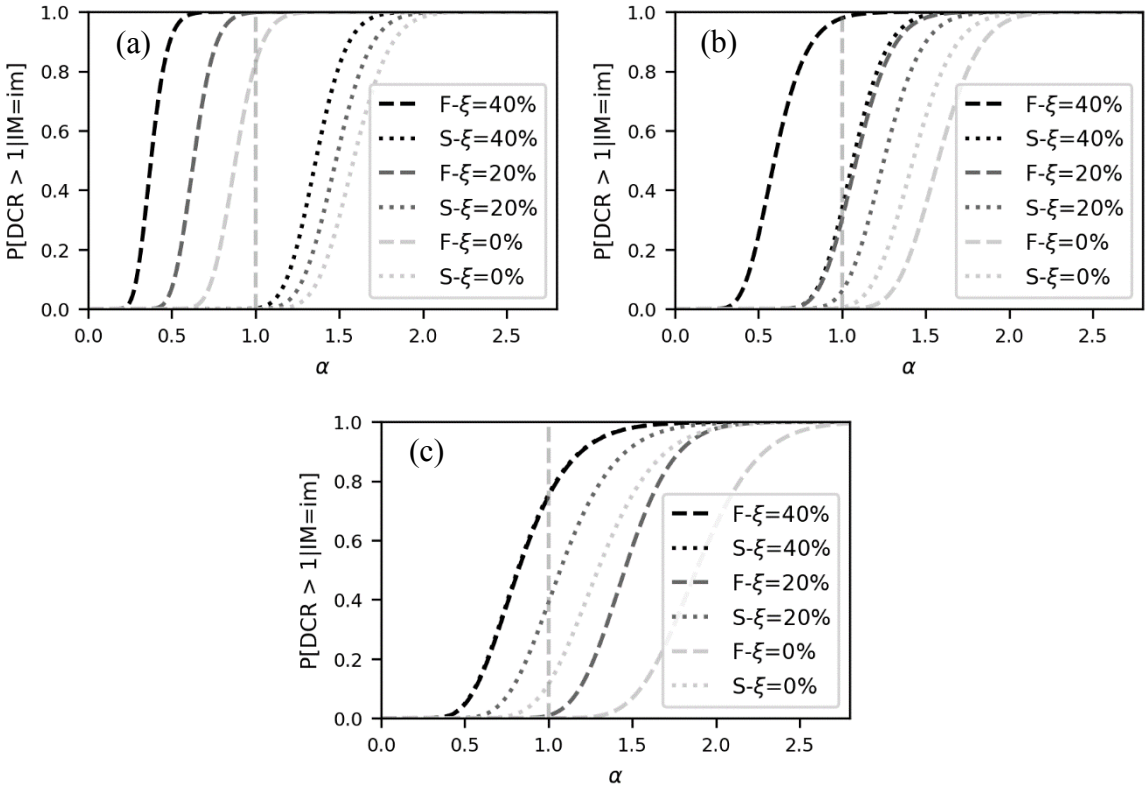

Figure 7: Flexural and shear fragility curves for five-beam bridge type, (a) 15 m-, (b) 35 m- and (c) 55 m-span. F: flexure; S: shear

In general, one can state that the variation of the geometric and mechanical characteristics analysed in this study does not strongly influence the response of the structure as fragility curves show low values of dispersion in most of the cases, while the state of prestressing tendon corrosion is much more decisive. This suggests, with a view to prioritisation during

bridge inspections, to focus attention and available resources on the state of prestressing tendons, which is fundamental for the response, while an investigation of the remaining characteristics could only be considered at a later stage. In addition, the study shows a greater vulnerability for short-span bridge typology, a consideration, however, to be validated with further investigation in future.

5 CONCLUSIONS

The fragility of prestressed concrete girder bridges subjected to traffic loads considering tendon corrosion is investigated in this study. A probabilistic assessment methodology is presented to evaluate the failure probability under traffic loads. The probabilistic assessment considers the influence of epistemic uncertainty on selected geometric and structural parameters which are unknown to operators during preliminary bridge assessment. The propagation of uncertainty is considered through statistical sampling techniques. In this study, the methodology is used to investigate the failure probability of nine prestressed concrete bridge superstructure typologies. Results show that particular attention should be given to the short-span typology which, according to the variable modelling choices adopted in this study, exhibits the weakest resistance to traffic loads, modelled as Italian code [25]. Variation of span length tends to considerably alter bridge fragility, particularly for short-span typology, leading up to a maximum of 56% of decrease in load-bearing capacity compared to the long-span one. The same cannot be stated for the beam number of the deck, which appears not to significantly affect the results, with a 10% of increase in the fragility curve median on average as the beam number increases, and a maximum value of 19% only in case of a short-span typology. Investigation on the influence of corrosion level for diverse span lengths and beam numbers leads to the conclusion that there is no need for particular attention to corrosion level for a specific bridge typology. Corrosion level is equally important for every investigated bridge typology and significantly affects the fragility, up to a decrease of 60% in load-bearing capacity for increasing corrosion level from 0 to 40%. Besides, for the long-span typology, results show a greater dispersion in fragility curves. This might be related to a larger variability of beam height and deck width for this particular bridge typology. To reduce this uncertainty in the fragility, as for validating the results obtained for the short-span typology, implementing simulated design in the procedure should be helpful. Finally, results prove that the flexural response governs the failure of the short-span bridge typology, compared to shear behaviour. The same applies to all the bridge typologies in presence of severe corrosion degree, thus leading to a ductile mechanism. On the other hand, this cannot be stated for low corrosion values for medium- and long-span bridge typologies, as brittle shear failure tends to be the most likely mechanism. The tendon corrosion involves a considerable loss of bridge flexural capacity. The achieved preliminary results can be adopted to guide operators for cases within the investigated bridge typologies. However, the same methodology can be similarly applied for investigating other case-study bridges in practice. Additional studies are needed, to evaluate the approximations related to the initial simplification assumptions on the adopted methodology for structural analysis. Finally, further developments should be aimed to analyse the probability of failure of other case-study bridges representative of existing typologies to be used by transport authority's operators for risk-based prioritisation purposes.

ACKNOWLEDGEMENTS

The third author acknowledges funding by Italian Ministry of University and Research, within the project 'PON-Ricerca e Innovazione-2014–2020, CUP Code (D.M. 10/08/2021, n. 1062): D95F21002140006. The last author acknowledges funding by Centro Nazionale

Sustainable Mobility Center, within the framework of MOST project, CUP code: D93C22000410001.

REFERENCES

[1] G. M. Calvi *et al.*, 'Once upon a Time in Italy: The Tale of the Morandi Bridge', *Structural Engineering International*, vol. 29, no. 2, pp. 198–217, Apr. 2019, doi: 10.1080/10168664.2018.1558033.

[2] F. Bazzucchi, L. Restuccia, and G. A. Ferro, 'Considerations over the Italian road bridge infrastructure safety after the polcevera viaduct collapse: Past errors and future perspectives', *Frattura ed Integrita Strutturale*, vol. 12, no. 46, pp. 400–421, Oct. 2018, doi: 10.3221/IGF-ESIS.46.37.

[3] A. Nettis, P. Iacovazzo, D. Raffaele, G. Uva, and J. M. Adam, 'Displacement-based seismic performance assessment of multi-span steel truss bridges', *Eng Struct*, vol. 254, Mar. 2022, doi: 10.1016/j.engstruct.2021.113832.

[4] S. P. Stefanidou and A. J. Kappos, 'Methodology for the development of bridge-specific fragility curves', *Earthq Eng Struct Dyn*, vol. 46, no. 1, pp. 73–93, Jan. 2017, doi: 10.1002/eqe.2774.

[5] A. Anisha, A. Jacob, R. Davis, and S. Mangalathu, 'Fragility functions for highway RC bridge under various flood scenarios', *Eng Struct*, vol. 260, Jun. 2022, doi: 10.1016/j.engstruct.2022.114244.

[6] G. Fiorillo and M. Ghosn, 'Fragility analysis of bridges due to overweight traffic load', *Structure and Infrastructure Engineering*, vol. 14, no. 5, pp. 619–633, May 2018, doi: 10.1080/15732479.2017.1380675.

[7] G. Miluccio, D. Losanno, F. Parisi, and E. Cosenza, 'Traffic-load fragility models for prestressed concrete girder decks of existing Italian highway bridges', *Eng Struct*, vol. 249, Dec. 2021, doi: 10.1016/j.engstruct.2021.113367.

[8] V. Sangiorgio, A. Nettis, G. Uva, F. Pellegrino, H. Varum, and J. M. Adam, 'Analytical fault tree and diagnostic aids for the preservation of historical steel truss bridges', *Eng Fail Anal*, vol. 133, Mar. 2022, doi: 10.1016/j.engfailanal.2021.105996.

[9] A. M. Abdallah, R. A. Atadero, and M. E. Ozbek, 'A State-of-the-Art Review of Bridge Inspection Planning: Current Situation and Future Needs', *Journal of Bridge Engineering*, vol. 27, no. 2, Feb. 2022, doi: 10.1061/(ASCE)BE.1943-5592.0001812.

[10] D. Y. Yang and D. M. Frangopol, 'Life-cycle management of deteriorating bridge networks with network-level risk bounds and system reliability analysis', *Structural Safety*, vol. 83, Mar. 2020, doi: 10.1016/j.strusafe.2019.101911.

[11] G. A. Ferro, L. Restuccia, D. Falliano, A. Devitofranceschi, and A. Gemelli, 'Collapse of Existing Bridges: From the Lesson of La Reale Viaduct to the Definition of a Partial Safety Coefficient of Variable Traffic Loads', *Journal of Structural Engineering*, vol. 148, no. 11, Nov. 2022, doi: 10.1061/(ASCE)ST.1943-541X.0003458.

[12] L. Anania, A. Badalà, and G. D'Agata, 'Damage and collapse mode of existing post tensioned precast concrete bridge: The case of Petrulla viaduct', *Eng Struct*, vol. 162, pp. 226–244, May 2018, doi: 10.1016/j.engstruct.2018.02.039.

[13] Ministero delle Infrastrutture e dei Trasporti, 'Linee guida per la classificazione e gestione del rischio, la valutazione della sicurezza ed il monitoraggio dei ponti esistenti.' 2020.

[14] FHWA - Office of Research Development and Technology, 'Guidelines for Sampling, Assessing, and Restoring Defective Grout in Prestressed Concrete Bridge Post-Tensioning Ducts.', 2013.
[15] A. Nettis, M. Saponaro, and M. Nanna, 'RPAS-based framework for simplified seismic risk assessment of Italian RC-bridges', *Buildings*, vol. 10, no. 9, Sep. 2020, doi: 10.3390/BUILDINGS10090150.
[16] B. A. Bradley, 'Epistemic uncertainties in component fragility functions', *Earthquake Spectra*, vol. 26, no. 1, pp. 41–62, 2010, doi: 10.1193/1.3281681.
[17] C. Zelaschi, R. Monteiro, and R. Pinho, 'Parametric Characterization of RC Bridges for Seismic Assessment Purposes', *Structures*, vol. 7, pp. 14–24, Aug. 2016, doi: 10.1016/j.istruc.2016.04.003.
[18] L. Jacinto, M. Pipa, L. A. C. Neves, and L. O. Santos, 'Probabilistic models for mechanical properties of prestressing strands', *Constr Build Mater*, vol. 36, pp. 84–89, Nov. 2012, doi: 10.1016/j.conbuildmat.2012.04.121.
[19] R. L. Iman and W. J. Conover, 'A Distribution-Free Approach to Inducing Rank Correlation Among Input Variables', *Commun Stat Simul Comput*, vol. 11, no. 3, pp. 311–334, Jan. 1982, doi: 10.1080/03610918208812265.
[20] D. H. Tavares, J. E. Padgett, and P. Paultre, 'Fragility curves of typical as-built highway bridges in eastern Canada', *Eng Struct*, vol. 40, pp. 107–118, Jul. 2012, doi: 10.1016/j.engstruct.2012.02.019.
[21] R. Monteiro, 'Sampling based numerical seismic assessment of continuous span RC bridges', *Eng Struct*, vol. 118, pp. 407–420, Jul. 2016, doi: 10.1016/j.engstruct.2016.03.068.
[22] V. Silva, H. Crowley, H. Varum, R. Pinho, and R. Sousa, 'Evaluation of analytical methodologies used to derive vulnerability functions', *Earthq Eng Struct Dyn*, vol. 43, no. 2, pp. 181–204, 2014, doi: 10.1002/eqe.2337.
[23] G. Albenga, *Lezioni di ponti*. Torino: U.T.E.T., 1930.
[24] CEN, 'Eurocode 1: Actions on structures - Part 2: Traffic loads on bridges', vol. EN 1991-2. Brussels, Belgium, 2003.
[25] Ministero delle Infrastrutture e dei Trasporti, 'Decreto Ministeriale 17 Gennaio 2018. Aggiornamento delle norme tecniche per le costruzioni. Gazzetta ufficiale n.42 del 20 febbraio 2018.' 2018.
[26] CEN, 'Eurocode 2: Design of concrete structures - Part 1-1 : General rules and rules for buildings.', vol. EN 1992-1-1. Brussels, Belgium, 2004.
[27] Q. Q. Yu, X. L. Gu, Y. H. Zeng, and W. P. Zhang, 'Flexural behavior of Corrosion-Damaged prestressed concrete beams', *Eng Struct*, vol. 272, Dec. 2022, doi: 10.1016/j.engstruct.2022.114985.
[28] J. W. Baker, 'Efficient analytical fragility function fitting using dynamic structural analysis', *Earthquake Spectra*, vol. 31, no. 1, pp. 579–599, Feb. 2015, doi: 10.1193/021113EQS025M.
[29] Ministero delle Infrastrutture e dei Trasporti, 'Circolare n.384 del 14.02.1962, Norme relative ai carichi per il calcolo dei ponti stradali.' 1962.